

# Effect of substrate on electroplated copper sulphide thin films

B. Bharathi · S. Thanikaikarasan · Pratap Kollu ·  
P. V. Chandrasekar · K. Sankaranarayanan ·  
X. Sahaya Shajan

Received: 23 May 2014 / Accepted: 2 September 2014 / Published online: 21 September 2014  
© Springer Science+Business Media New York 2014

**Abstract** Copper Sulphide thin films have been prepared on different substrates using electrodeposition technique. X-ray diffraction analysis showed that the prepared films possess polycrystalline in nature with cubic structure. Microstructural parameters such as crystallite size, strain and dislocation density are determined using X-ray diffraction data. Film composition and surface morphology have been analyzed using Scanning electron microscopy and Energy dispersive analysis by X-rays. Optical absorption analysis showed that the prepared films possess band gap value in the range between 2.2 and 2.4 eV for films obtained on different substrates.

## 1 Introduction

Metal Chalcogenides have found numerous applications in variety of solid state devices such as optical devices and

solar cells [1, 2]. Copper Sulphides ( $\text{Cu}_x\text{S}$ ,  $x = 1-2$ ) is found to be as significant binary compound which have been found number of applications such as solar absorber coatings for photothermal conversion of solar energy and filters for selective radiations on architectural windows [3, 4]. Copper Sulphides are found to exist in five non-stoichiometric and mixed phases at room temperature viz., covellite ( $\text{CuS}$ ) in “sulphur-rich region” and anilite ( $\text{Cu}_{1.75}\text{S}$ ), digenite ( $\text{Cu}_{1.8}\text{S}$ ), djurleite ( $\text{Cu}_{1.95}\text{S}$ ), and chalcocite ( $\text{Cu}_2\text{S}$ ) in “copper-rich region” [5]. Among them,  $\text{Cu}_2\text{S}$  is found to be a *p*-type semiconductor with an energy gap value in the range between 1.2 and 1.93 eV which make them interesting for energy conversion through electrochemical route [6–8]. Polycrystalline Copper Sulphide ( $\text{Cu}_2\text{S}$ ) thin films are usually crystallized in cubic structure (JCPDS ICDD 2003, File No. 65-2980). Number of techniques have been reported for the preparation of  $\text{Cu}_2\text{S}$  thin films with device quality such as, thermal evaporation [9], RF reactive sputtering [10], hydrothermal technique [11], microwave assisted chemical bath deposition [12], chemical vapour deposition [13], successive ionic layer adsorption and reaction technique [14], atomic layer deposition [15], spraypyrolysis [16]. Among them, electrodeposition is one of the appropriate methods to prepare good quality films. It seems to be attractive due to its simplicity, low temperature processing, low cost of synthesize, control of film thickness and morphology by readily adjusting the deposition parameters as well as composition of the electrolytic bath, etc. [17, 18].

In the present work, thin films of  $\text{Cu}_2\text{S}$  have been prepared on various substrates such as tin oxide coated conducting glass ( $\text{SnO}_2$ ) substrates, fluorine doped tin oxide coated conducting glass substrates ( $\text{SnO}_2:\text{F}$ ) and indium doped tin oxide coated conducting glass substrates ( $\text{SnO}_2:\text{In}$ ). The deposition mechanism has been analyzed using cyclic

---

B. Bharathi · S. Thanikaikarasan (✉) · P. V. Chandrasekar ·  
X. S. Shajan  
Centre for Scientific and Applied Research, School of Basic  
Engineering and Sciences, PSN College of Engineering and  
Technology, Tirunelveli 627 152, Tamil Nadu, India  
e-mail: s\_thanikai@rediffmail.com

P. Kollu  
Department of Metallurgical Engineering and Materials Science,  
DST-INSPIRE Faculty, Indian Institute of Technology,  
Mumbai 400 076, Maharashtra, India

P. V. Chandrasekar  
Institute of Optoelectronic Display, Fuzhou University,  
Fuzhou 350 002, Republic of China

K. Sankaranarayanan  
School of Physics, Alagappa University,  
Karaikudi 630 004, Tamil Nadu, India

voltammetry. Prepared films have been subjected to X-ray diffraction (XRD), Scanning electron microscopy (SEM), Energy dispersive analysis by X-rays (EDX) and Optical absorption analysis (UV–Vis–NIR) techniques, respectively. The effect of substrate on electrochemical, microstructural, morphological, compositional and optical properties of the deposited films are analyzed. The experimental observations are discussed in detail.

## 2 Experiment

### 2.1 Experimental details

The chemicals used in the present work were of AR grade (99.5 % purity, Merck). Cu<sub>2</sub>S thin films were deposited on SnO<sub>2</sub>:F, SnO<sub>2</sub> and SnO<sub>2</sub>:In (sheet resistance 20 ohms/square) substrates from an aqueous acidic bath containing 0.05 M CuSO<sub>4</sub> and 0.05 M Na<sub>2</sub>S<sub>2</sub>O<sub>3</sub>. The first working solution was obtained by dissolving 1.2489 g CuSO<sub>4</sub> in 100 cc deionized water and the second working solution Na<sub>2</sub>S<sub>2</sub>O<sub>3</sub> was obtained by dissolving 1.2409 g Na<sub>2</sub>S<sub>2</sub>O<sub>3</sub> in 100 cc of deionized water. Each 20 cc of the two solutions forms the reaction mixture and this mixture was used as an electrolytic bath for all depositions. Before, used for deposition process the substrates were treated with ultrasonic waves in a bath of methanol for 15 min and then rinsed with acetone followed by double distilled water. Initially, the pH of the electrolytic bath was maintained at 4.0 ± 0.1. By adding an adjustable amount of H<sub>2</sub>SO<sub>4</sub>, the pH value was adjusted to 2.0 ± 0.1. The pH value was fixed as 2.0 ± 0.1 for all depositions. The depositions were carried out using SP50 Potentiostat/Galvanostat Unit (Bio Logic, France) employing three electrode cell configuration with SnO<sub>2</sub>, SnO<sub>2</sub>:F and SnO<sub>2</sub>:In substrates as cathode, graphite plate as anode and saturated calomel electrode (SCE) as reference electrode, respectively. The SCE was introduced into the solution by Luggin capillary arrangement whose tip was placed as close as possible to the working electrode. The experimental potential was measured with respect to SCE. The electrolytic processes were monitored by cyclic voltammetry and governed potentiostatically. The deposition potential and bath temperature were fixed as –1000 mV versus SCE and 60 °C. The deposition time was found to be vary in the range between 5 and 60 min.

### 2.2 Characterization

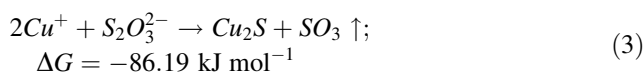
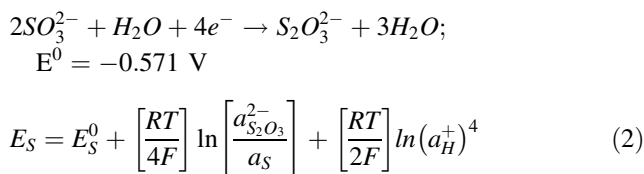
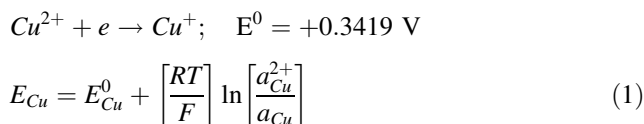
In situ characterization technique such as cyclic voltammetry was carried out to fix the deposition potential of the deposited films. Thickness of the prepared films was estimated using Stylus Profilometer (Mitutoyo SJ 301, Japan). X-ray diffraction data of the prepared films was taken out

using an X-ray diffractometer (X'PERT PRO PANalytical X-ray diffractometer, Netherland) with CuK<sub>α</sub> radiation (λ = 1.5406 Å). Surface morphology and film composition were analyzed using an Energy dispersive analysis by X-rays set up attached with Scanning electron microscope (JEOL JSM 840). Optical absorption analysis was carried out using (Shimadzu Model 2600, Singapore) UV–Vis–NIR spectrophotometer.

## 3 Results and discussion

### 3.1 Cyclic voltammetry

The formation of alloy in electrodeposition process is more complex, because they involve several thermodynamic problems such as poor adhesion of film to the substrates due hydrogen evolution, more acidic nature and peel off film from the substrate. The formation of Cu<sub>2</sub>S thin film in electrodeposition process, the deposition of less noble constituent (here formation of metallic alloy S) takes place first at potential which is quite closer to standard reduction potential of S<sub>2</sub>O<sub>3</sub><sup>2-</sup> according to Eq. (2). Cu<sub>2</sub>S thin films are formed according to Eq's as mentioned below from Eqs. (1) to (3).



where E<sub>Cu</sub> and E<sub>S</sub> are potential of the working electrode in a given solution. E<sub>Cu</sub><sup>0</sup>, E<sub>S</sub><sup>0</sup> are the standard electrode potential for Cu and S respectively with respect to SCE. R is universal gas constant, T is absolute temperature of the electrolytic bath, N is the number of electrons required for the reduction and F is Faraday constant. a<sub>Cu</sub><sup>2+</sup>, a<sub>S<sub>2</sub>O<sub>3</sub><sup>2-</sup></sub> are the activities of Cu and S ions which are present in the electrolytic bath. a<sub>Cu</sub>, a<sub>S</sub> are the activities of respective atoms present in the deposited films. The deposition of Cu occurs at potentials more positive than their standard reduction potential by gaining free energy in the compound formation. The formation of Cu<sub>2</sub>S thin films takes place with negative free energy ΔG = –86.19 kJ mol<sup>-1</sup>. Cyclic voltammetric studies have been carried out in a standard three compartment cell consisting of SnO<sub>2</sub>:F, SnO<sub>2</sub> and SnO<sub>2</sub>:In substrate as working electrode, graphite electrode as counter electrode and SCE as

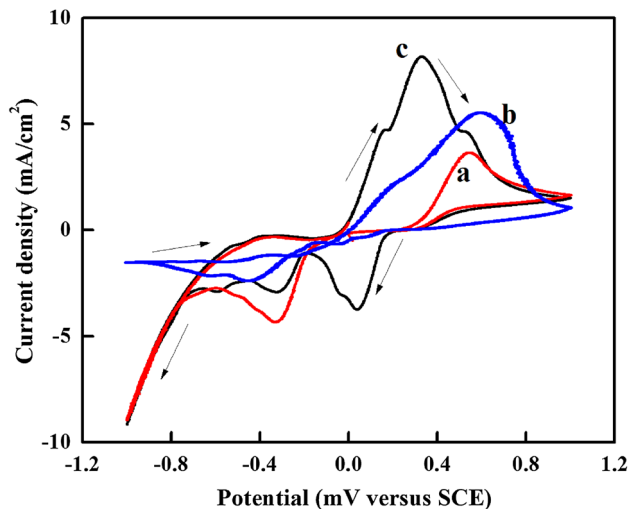


**Fig. 1** Cyclic voltammogram of  $\text{Cu}_2\text{S}$  thin film obtained from an aqueous electrolytic bath consisting of 0.05 M  $\text{CuSO}_4$  and 0.05 M  $\text{Na}_2\text{S}_2\text{O}_3$ : (a)  $\text{SnO}_2\text{:F}$ , (b)  $\text{SnO}_2$  and (c)  $\text{SnO}_2\text{:In}$  substrate

reference electrode, respectively. The electrolytic bath consisting of 0.05 M  $\text{CuSO}_4$  and 0.05 M  $\text{Na}_2\text{S}_2\text{O}_3$ . The scan rate is fixed as  $20 \text{ mV s}^{-1}$  and the voltammetric curves are scanned in the potential range between  $-1,000 \text{ mV}$  and  $+1,000 \text{ mV}$  versus SCE. Figure 1a shows cyclic voltammogram recorded for  $\text{SnO}_2$  substrate obtained from an acidic bath containing 0.05 M  $\text{CuSO}_4$  and 0.05 M  $\text{Na}_2\text{S}_2\text{O}_3$ . During positive scan, observation of oxidation peak at  $+540 \text{ mV}$  versus SCE may be due to oxidation of  $\text{Cu}^{2+}$  to  $\text{Cu}^+$ . Reduction peak I observed at  $-325 \text{ mV}$  versus SCE may be due to the formation of  $\text{Cu}_2\text{S}$  film on  $\text{SnO}_2$  substrate according to Eq. (3). Also, observation of peak at  $+39 \text{ mV}$  versus SCE may be due to reduction of solvent present in the electrolytic bath. Similar behaviour is exhibited for films obtained on  $\text{SnO}_2\text{:F}$  substrate which is indicated in Fig. 1b. Cyclic voltammogram recorded for  $\text{SnO}_2\text{:In}$  substrate obtained from an acidic bath containing 0.05 M  $\text{CuSO}_4$  and 0.05 M  $\text{Na}_2\text{S}_2\text{O}_3$  which is shown in Fig. 1c. Cathodic current density increases gradually up to  $+325 \text{ mV}$  versus SCE substrate which may be due to the formation of  $\text{Cu}^+$  ion from an electrolytic bath. The observation of peak at  $+39 \text{ mV}$  versus SCE may be due to reduction of solvent. Reduction peak appeared at  $-325 \text{ mV}$  versus SCE may be due to the formation of  $\text{Cu}_2\text{S}$  films on  $\text{SnO}_2\text{:In}$  substrate according to Eq. (3). A slight shift in deposition potential observed in the present work which may be due to the usage of different substrates [19]. Different deposition potentials are observed for  $\text{Cu}_2\text{S}$  thin films have been reported earlier [20].

### 3.2 Film thickness

Thickness of the deposited films is controlled by two separate variables such as (1) uniform growth and (2)

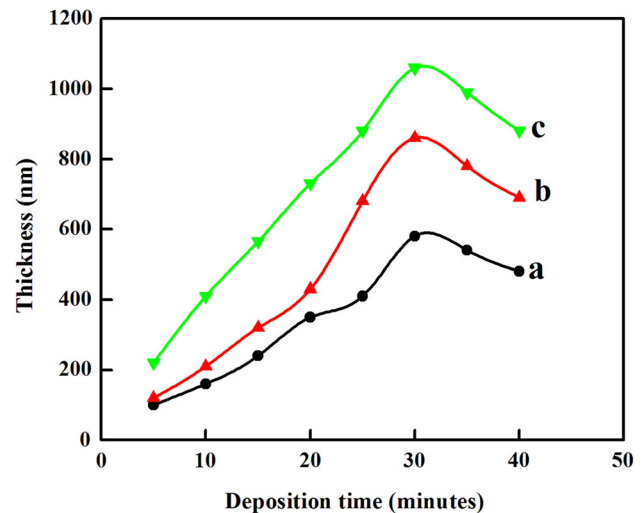


**Fig. 2** Variation of film thickness with deposition time for  $\text{Cu}_2\text{S}$  thin films obtained on different substrates: (a)  $\text{SnO}_2\text{:F}$ , (b)  $\text{SnO}_2$  (c)  $\text{SnO}_2\text{:In}$

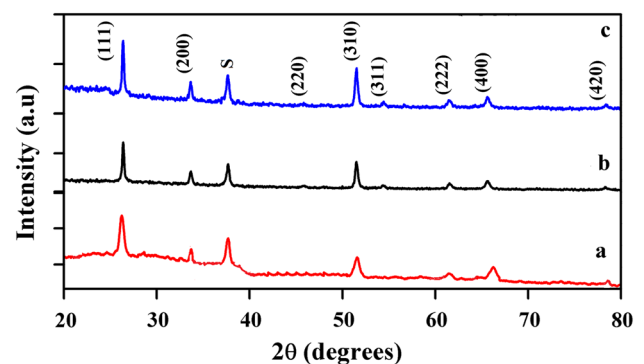


**Fig. 3** X-ray diffraction pattern recorded for  $\text{Cu}_2\text{S}$  thin films obtained on different substrates: (a)  $\text{SnO}_2\text{:F}$ , (b)  $\text{SnO}_2$  (c)  $\text{SnO}_2\text{:In}$

surface morphology [21]. Thickness of the deposited films are controlled by controlling the deposition potential, plating current, plating time and usage of various substrate and bath temperature. Thickness of the deposited films is measured using stylus profilometer. Figure 2a–c shows the variation of film thickness with deposition time for films obtained on different substrates such as  $\text{SnO}_2\text{:F}$ ,  $\text{SnO}_2$  and  $\text{SnO}_2\text{:In}$ . It is observed that film thickness increases linearly with deposition time and reaches its maximum value at a deposition time of 30 min for films prepared on  $\text{SnO}_2\text{:F}$  substrate (Fig. 2a). Similar behaviour is exhibited for films obtained on different substrates such as  $\text{SnO}_2$  and  $\text{SnO}_2\text{:In}$  in which is indicated in Fig. 2b, c. Decrease in film thickness value after certain intervals of time (after 30 min) which may be due higher rate of dissolution than rate of deposition [21]. Films with higher thickness (1,060 nm) is

obtained at a deposition time of 30 min for films obtained on SnO<sub>2</sub>:In substrate. Therefore, SnO<sub>2</sub>:In is used as best substrate to obtain films with higher thickness values.

### 3.3 X-ray diffraction

X-ray diffraction pattern of Cu<sub>2</sub>S thin films deposited on different substrates is shown in Fig. 3. XRD patterns showed that the deposited films are found to exhibit cubic structure. All the identified peaks are from Cu<sub>2</sub>S phase. The different peaks in the diffractogram are indexed and the corresponding values of interplanar spacing “d” are calculated and compared with standard JCPDS ICDD file for cubic Cu<sub>2</sub>S [22]. The appearance of peak at 2θ value corresponds to metallic Sulphur present in the deposited films [23]. The observation of slight shift in peak intensity may due to usage of different substrates. The height of (111) peak is found to be higher than all other peaks in the XRD pattern indicated that the crystallites are preferentially oriented along (111) plane. Though, the peak intensities are slightly varied but no other changes are observed in all identified diffraction patterns. The presence of sharp and more intense diffraction peaks for films obtained on SnO<sub>2</sub>:In substrate correspond to the formation of films with better crystallinity. The crystallite size value of the deposited films is calculated using FWHM data which must be obtained from XRD pattern and Debye–Scherrer formula [24].

$$D = \frac{0.9\lambda}{\beta \cos \theta} \tag{4}$$

where λ is the wavelength of CuK<sub>α</sub> target used (λ = 1.5406 Å), β is full width at half maximum of the peak position in radian, θ is Bragg’s diffraction angle at peak position in degree. Strain is defined as the force which can be act on the surface of the film to restrict the formation of crystallites on its surface [17]. The value of strain (ε) is calculated using Williamson Hall plot analysis method by using Eq. (5).

$$\beta = \left[ \frac{\lambda}{D \cos \theta} - \varepsilon \tan \theta \right] \tag{5}$$

Dislocation density (δ) is defined as the number of dislocation lines per unit volume of the crystal and its value is calculated by using Eq. (6) [24].

$$\delta = \frac{1}{D^2} \tag{6}$$

The value of crystallite size is controlled by the usage of different substrates. It is noted that, films with higher thickness value having lower crystallite size and lower thickness value having higher crystallite size may be due to the quantum confinement effect produced by the usage of various substrates [25]. The value of microstructural parameters such as crystallite size, strain and dislocation density are calculated using XRD data and given in Table 1. The value of strain, dislocation density and film thickness are found to be smaller than films obtained on SnO<sub>2</sub>:In substrate. The crystallite size value for films obtained on SnO<sub>2</sub>:In substrate is higher than value obtained on SnO<sub>2</sub> and SnO<sub>2</sub>:F substrate.

### 3.4 Morphological and compositional analyses

SEM images for films prepared on different substrates are recorded using scanning electron microscope. SEM images observed for films prepared on SnO<sub>2</sub>, SnO<sub>2</sub>:F and SnO<sub>2</sub>:In substrate are shown in Fig. 4a–c. The observation of slight change in surface morphology may be due to usage of different substrates [25]. The grains are found to be spherical in shape with non uniform surface coverage which is indicated in Fig. 4a. Similar morphological behaviour is exhibited for films which have been reported earlier [26]. It is observed from Fig. 4 b, c several crystallites are joined together to form grains. The average size of the grains are found to be 400, 320 nm for films obtained on SnO<sub>2</sub> and SnO<sub>2</sub>:In substrates. The film composition of the deposited films is analyzed using an EDX set up attached with SEM. The value of atomic percentage for films obtained on different substrates which is indicated in Table 1. It is observed from Table 1 that the deposited films has atomic percentage value (Cu:S) 71.90:29.10, (Cu:S) 69.18:30.82 for films obtained on SnO<sub>2</sub> and SnO<sub>2</sub>:In. The atomic molar ratio (Cu:S) for films obtained

**Table 1** Microstructural parameters, atomic percentage and band gap value of Cu<sub>2</sub>S thin film obtained on different substrates: (a) SnO<sub>2</sub>:F, (b) SnO<sub>2</sub> and (c) SnO<sub>2</sub>:In

Sl. no.	Substrate	Film thickness (nm)	Crystallite size (D), (nm)	Dislocation density (δ), lines m <sup>-2</sup> × 10 <sup>14</sup>	Strain (ε), lines <sup>-2</sup> m <sup>-4</sup> × 10 <sup>-3</sup>	Bandgap (E <sub>g</sub> ), (eV)	Atomic percentage (%)	
							Cu	S
1.	SnO <sub>2</sub> :F	580	48.77	5.91	68.3	2.39	71.52	28.48
2.	SnO <sub>2</sub>	860	52.39	3.50	61.9	2.31	70.90	29.10
3.	SnO <sub>2</sub> :In	1,060	59.72	2.80	15.1	2.20	69.18	30.82



on SnO<sub>2</sub>:In substrate is found to be 1.80:0.92 indicated that the deposited is nearly stoichiometric. This result is consistent with X-ray diffraction analysis of the sample with phase corresponds to Cu<sub>2</sub>S. Increase in value of Cu and decrease in value of S may be due to cumulative effect of ionic transport, discharge, nucleation, growth of Sulphur at higher concentration.

### 3.5 Optical absorption analysis

The change in value of optical transmittance of the deposited films may be due to usage of different substrates [25]. Transmittance spectra recorded for Cu<sub>2</sub>S thin films obtained on SnO<sub>2</sub>:F, SnO<sub>2</sub> and SnO<sub>2</sub>:In substrates are shown in Fig. 5a–c. It is observed that the film deposited on SnO<sub>2</sub> substrate has showed maximum transmittance in visible region. The value of absorption coefficient is calculated using Eq. (7) [18]

$$\alpha = \frac{1}{t} \ln \left( \frac{A}{T} \right) \quad (7)$$

where  $\alpha$  is the absorption coefficient in cm<sup>-1</sup>,  $t$  is thickness value of the film in nm,  $A$  is absorbance and  $T$  is transmittance percentage. The nature of transition present in the deposited films which is determined using the following Eq. (8) [17]

$$\alpha h\nu = A(h\nu - E_g)^n \quad (8)$$

where  $h\nu$  is photon energy in eV,  $E_g$  is an energy gap in eV,  $A$  is an energy dependent constant and  $n$  is an integer. The percentage value of absorption and transmittance for films obtained on different substrates are carried out to determine optical properties of the deposited films. A plot of  $(h\nu)$  versus  $(\alpha h\nu)^2$  for Cu<sub>2</sub>S thin films obtained on different substrates are indicated by curves a, b, c which is shown in Fig. 6. The observation showed that the plot is linear indicating the presence of direct transition in the deposited films. Extrapolation of linear portion of the plot to energy  $(h\nu)$  axis gives the band gap value of the deposited films. The band gap value of the deposited film are found to be 2.39, 2.31 and 2.20 eV for films obtained on SnO<sub>2</sub>:F, SnO<sub>2</sub> for SnO<sub>2</sub>:In substrates. Variation in band gap value of the deposited films may be due to usage of different substrates [25]. The band gap value obtained in the present work must be closer to the value reported earlier [26]. The value of extinction coefficient and refractive index are determined using Eqs. (9) and (10). Figure 7 shows the variation of refractive index ( $n$ ) with wavelength ( $\lambda$ ) for Cu<sub>2</sub>S thin films prepared on various substrates. It is observed that the value of ( $n$ ) decreases with ( $\lambda$ ) for films obtained on SnO<sub>2</sub>:F, SnO<sub>2</sub>:In, SnO<sub>2</sub> substrates. Variation of extinction coefficient ( $k$ ) with wavelength ( $\lambda$ ) for Cu<sub>2</sub>S thin films prepared

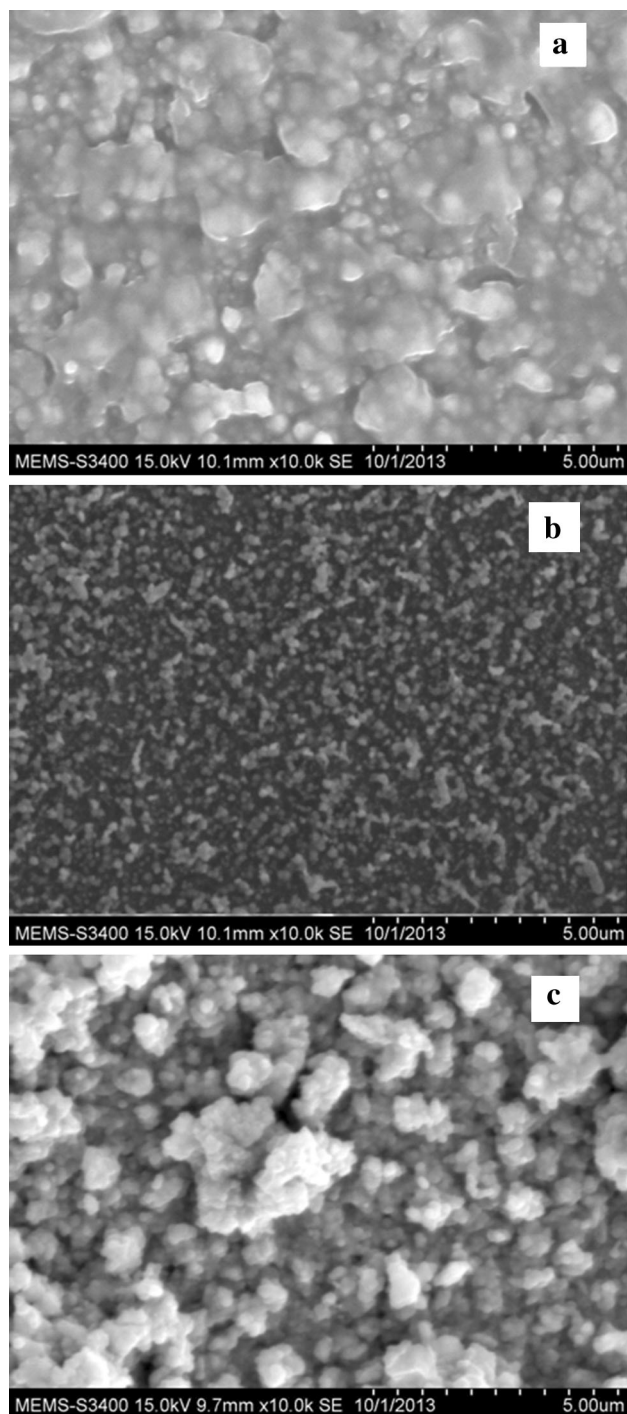


**Fig. 4** SEM images of Cu<sub>2</sub>S thin film obtained on different substrates: (a) SnO<sub>2</sub>:F, (b) SnO<sub>2</sub> (c) SnO<sub>2</sub>:In

on different substrates is shown in Fig. 8. It is observed that the value of ( $k$ ) decreases with respect to  $\lambda$  for all substrates. The value of real and imaginary dielectric constants are determined using Eqs. (11) and (12). Variation of real and imaginary part of dielectric constants ( $\epsilon_1$  and  $\epsilon_2$ ) with respect to wavelength ( $\lambda$ ) for Cu<sub>2</sub>S thin films obtained on different substrates is shown in Figs. 9 and 10.

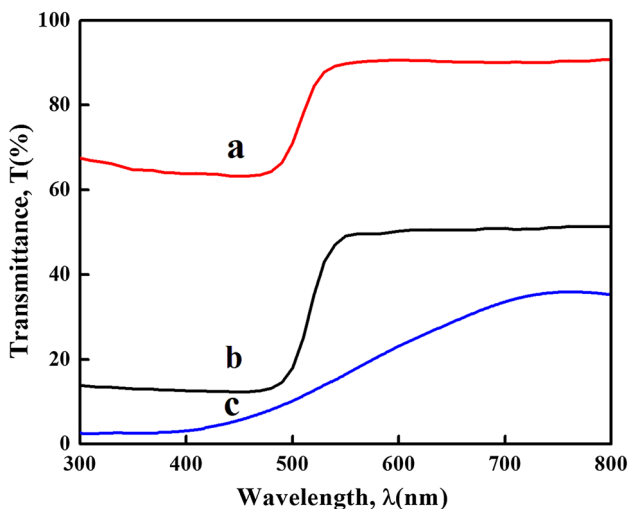


**Fig. 5** Transmittance spectra recorded for Cu<sub>2</sub>S thin films obtained on different substrates: (a) SnO<sub>2</sub>:F, (b) SnO<sub>2</sub> (c) SnO<sub>2</sub>:In

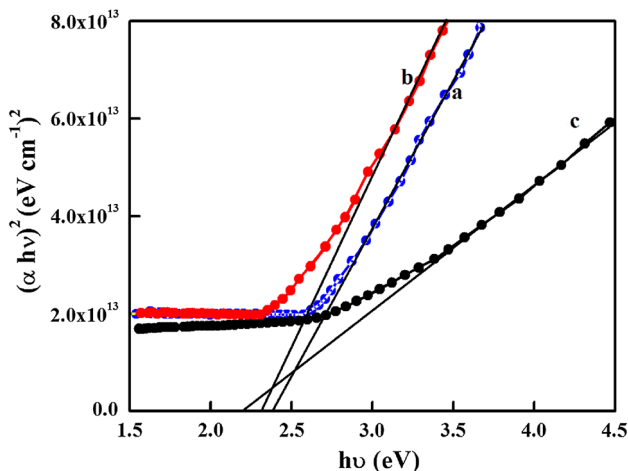


**Fig. 6** Plot of  $(\alpha h\nu)^2$  versus  $h\nu$  for Cu<sub>2</sub>S thin films on obtained on different substrates: (a) SnO<sub>2</sub>:F, (b) SnO<sub>2</sub> (c) SnO<sub>2</sub>:In

It is observed that both  $(\epsilon_1)$  and  $(\epsilon_2)$  are found to decrease with respect to  $(\lambda)$  for film obtained on SnO<sub>2</sub>:F, SnO<sub>2</sub> and SnO<sub>2</sub>:In substrates.

$$k = \frac{\alpha\lambda}{4\pi} \tag{9}$$

$$n = \left( \frac{1+R}{1-R} \right) - \sqrt{\frac{4R}{(1-R)^2} - k^2} \tag{10}$$

$$\epsilon_1 = n^2 - k^2 \tag{11}$$

$$\epsilon_2 = 2nk \tag{12}$$

**4 Conclusions**

Thin films of Cu<sub>2</sub>S thin films were prepared on different substrates such as SnO<sub>2</sub>:F, SnO<sub>2</sub> and SnO<sub>2</sub>:In using

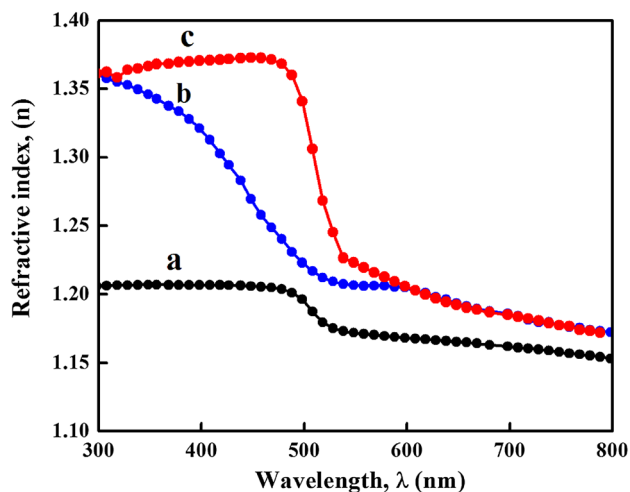


**Fig. 7** Variation of refractive index ( $n$ ) with wavelength ( $\lambda$ ) for Cu<sub>2</sub>S thin films obtained on different substrates: (a) SnO<sub>2</sub>:F, (b) SnO<sub>2</sub> (c) SnO<sub>2</sub>:In

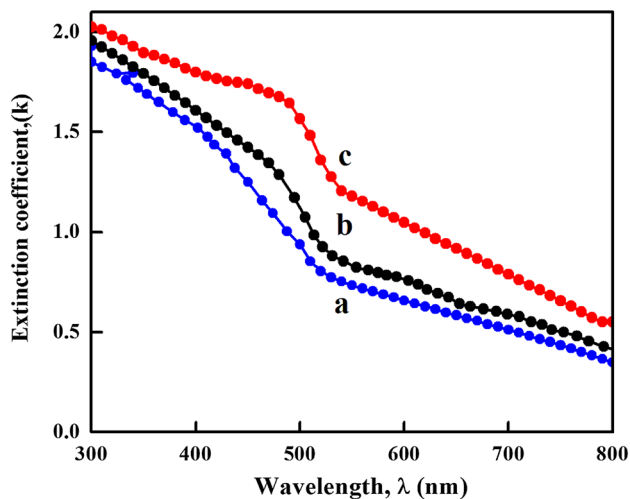


**Fig. 8** Variation of extinction coefficient ( $k$ ) with wavelength ( $\lambda$ ) for Cu<sub>2</sub>S thin films obtained on different substrates: (a) SnO<sub>2</sub>:F, (b) SnO<sub>2</sub> (c) SnO<sub>2</sub>:In substrate

electrodeposition technique. Structural analysis showed that the prepared films possess polycrystalline in nature with cubic structure with preferential orientation along (111) plane. Microstructural parameters estimated using Williamson Hall plot analysis were found to exhibit monotonic variation with respect to usage of different substrates. Film surface was found to be smooth with coverage of spherically shaped grains for films obtained on SnO<sub>2</sub>:In substrate. The band gap value was found to be in the range between 2.20 and 2.40 eV for films obtained on different substrates. Also, the optical parameters such as refractive index, extinction coefficient, real and imaginary

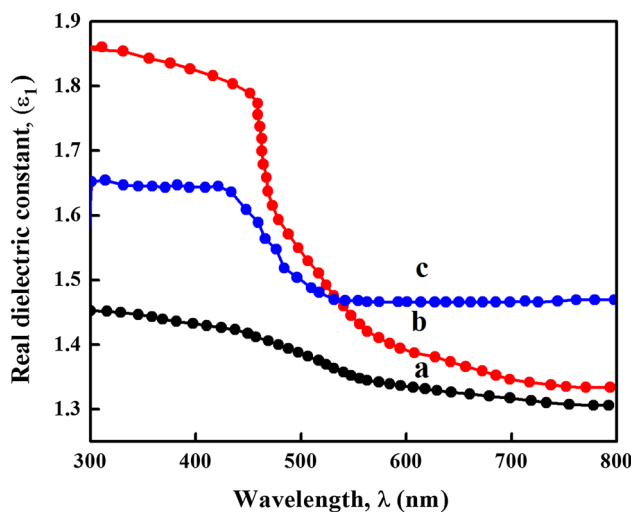


**Fig. 9** Variation of real dielectric constant ( $\epsilon_1$ ) with wavelength ( $\lambda$ ) for  $\text{Cu}_2\text{S}$  thin films obtained on different substrates: (a)  $\text{SnO}_2:\text{F}$ , (b)  $\text{SnO}_2$  (c)  $\text{SnO}_2:\text{In}$

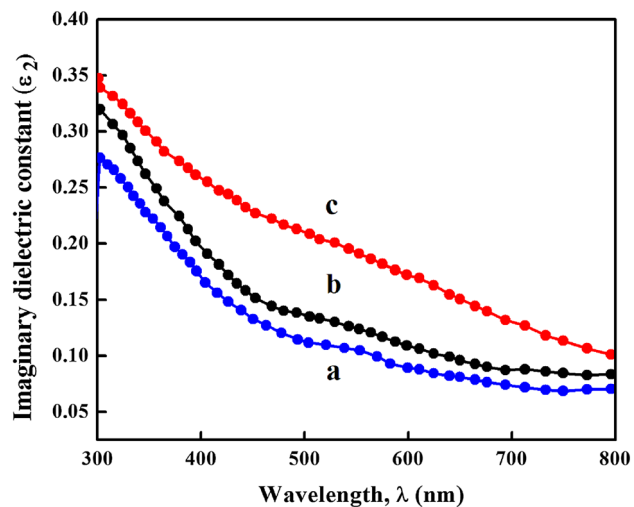


**Fig. 10** Variation of imaginary dielectric constant ( $\epsilon_2$ ) with wavelength ( $\lambda$ ) for  $\text{Cu}_2\text{S}$  thin films obtained on different substrates: (a)  $\text{SnO}_2:\text{F}$ , (b)  $\text{SnO}_2$  (c)  $\text{SnO}_2:\text{In}$

dielectric constant were determined. As a result, the films obtained on  $\text{SnO}_2:\text{In}$  substrate was found to exhibit well oriented properties than films obtained on some other substrates.

**Acknowledgments** The corresponding author Dr. S. Thanikaikarasan (Principal Investigator) and B. Bharathi (Junior Research Fellow) gratefully acknowledge the financial support received from the Board

of Research in Nuclear Sciences, Department of Atomic Energy (BRNS-DAE), Mumbai, India with File No. 2012/34/13/BRNS/No. 166 for carrying out this research work.

## References

1. Kirk-Othmer, *Encyclopedia of Chemical Technology*, vol. 20, (New York, 1982)
2. H. Moon, A. Kathalingam, T. Mahalingam, J.P. Chu, Y.D. Kim, *J. Mater. Sci.: Mater. Electron.* **18**, 1013 (2007)
3. P.K. Nair, V.M. Garca, A.M. Fernandez, H.S. Ruiz, M.T.S. Nair, *J. Phys. D: Appl. Phys.* **24**, 44 (1991)
4. P.J. Sebastain, O. Gomez-Daza, J. Campos, L. Banos, P.K. Nair, *Solar Energy Mater.* **32**, 159 (1994)
5. S. Djurle, *Acta Chem. Scand.* **12**, 1415 (1958)
6. M. Savelli, J. Bougnot, B.O. Seraphin. Solar energy conversion. in *Topics in Applied Physics*, vol. 31 (1979), p. 213
7. A.P. Alivisatos, *Science* **271**, 933 (1996)
8. M. Dachraoui, J. Vedel, *Solar Cells* **22**, 187 (1987)
9. H. Derin, *Appl. Phys. A* **114**, 838 (2014)
10. Y. He, W. Kriegseis, J. Blasing, A. Polity, T. Kramer, D. Hasselkamp, B.K. Meyer, M. Hardt, Alois Krost, *Jpn. J. Appl. Phys.* **41**, 4630 (2002)
11. F. Zhuge, X. Li, X. Gao, X. Gan, F. Zhou, *Mater. Lett.* **63**, 652 (2009)
12. M. Xin, K.W. Li, H. Wang, *Appl. Surf. Sci.* **256**, 1436 (2009)
13. M. Kemmler, M. Lazell, P.O. Brien, D.J. Otway, J.H. Park, J.R. Walsh, *J. Mater. Sci.: Mater. Electron.* **13**, 531 (2002)
14. L. Chen, Y. Zou, W. Qiu, F. Chen, M. Xu, M. Shi, H. Chen, *Thin Solid Films* **520**, 5249 (2012)
15. J. Johansson, J. Kostamo, M. Karppinen, L. Niinisto, *J. Mater. Chem.* **12**, 1022 (2002)
16. S.Y. Wang, W. Wang, Z.H. Lu, *Mater. Sci. Eng. B* **103**, 184 (2003)
17. S. Thanikaikarasan, X. Sahaya Shajan, V. Dhanasekaran, T. Mahalingam, *J. Mater. Sci.* **46**, 4034 (2011)
18. S. Thanikaikarasan, T. Mahalingam, *J. Alloys Compd.* **511**, 115 (2012)
19. T. Mahalingam, J.S.P. Chitra, S. Rajendran, P.J. Sebastian, *Semicond. Sci. Tech.* **17**, 565 (2002)
20. K. Anuar, Z. Zainal, M.Z. Hussein, H. Ismail, *J. Mater. Sci.: Mater. Electron.* **12**, 147 (2001)
21. T. Mahalingam, V.S. John, S. Rajendran, P.J. Sebastian, *Semicond. Sci. Tech.* **17**, 465 (2002)
22. Jointed Council for Powder Diffracted System International Centre for Diffraction Data 2003, PDF No. 65 2980, Pennsylvania, USA
23. Jointed Council for Powder Diffracted System International Centre for Diffraction Data 2003, PDF No. 20 1225, Pennsylvania, USA
24. S. Thanikaikarasan, T. Mahalingam, K. Sundaram, A. Kathalingam, Y. Deak Kim, T. Kim, *Vacuum* **83**, 1066 (2009)
25. V. Dhanasekaran, T. Mahalingam, *J. Alloy. Compd.* **539**, 50 (2012)
26. S.V. Bagul, S.D. Chavhan, R. Sharma, *J. Phys. Chem. Solids* **68**, 1623 (2007)